Alexandria Engineering Journal (2022) 61, 5371–5381

HOSTED BY

ELSEVIER

Alexandria University

Alexandria Engineering Journal

www.elsevier.com/locate/aej
www.sciencedirect.com

Numerical analysis of UFMC and FBMC in wavelength conversion for radio over fiber systems using semiconductor optical amplifier

Yazan Alkhlefat, Sevia M. Idrus [*,1], **Farabi M. Iqbal**

Universiti Teknologi Malaysia (UTM), Malaysia

Received 6 May 2021; revised 15 October 2021; accepted 30 October 2021
Available online 20 November 2021

KEYWORDS

5G;
Filtered bank multicarrier (FBMC);
Millimeter-wave (MMW);
Orthogonal frequency division multiplexing (OFDM);
Off-set quadrature amplitude (OQAM);
Out-of-band (OOB);
Peak to average power ratio (PAPR);
Semiconductor optical amplifier (SOA);
Sideband suppression ratio (SSR);
Universal filtered multicarrier (UFMC)

Abstract The 5G networks promise to use advanced access techniques and modulation formats to achieve new requirements of the huge number of users such as higher data, high speed, and low latency. Millimeter-wave (MMW) signal and new modulation schemes such as universal filtered multicarrier (UFMC) and filtered bank multicarrier (FBMC) are playing a fundamental role to accomplish these requirements. UFMC and FBMC are classified under multicarrier modulation formats which are considered as a suitable modulation scheme in 5G and replacing a well-known modulation format of filtered orthogonal frequency division multiplexing (OFDM) which was used in 4G. This interest in using UFMC and FBMC in 5G wireless systems is the reduction of out-of-band (OOB) spectrum in UFMC and reduction of sidelobe suppression in FBMC. The contribution of this paper is to propose a model of wavelength conversion using a semiconductor optical amplifier (SOA) for both schemes UFMC and FBMC- off-set quadrature amplitude (OQAM). In addition, we analyze and compare their performance in terms of bit error rate (BER) and error vector magnitude (EVM) for a wavelength conversion application. Finally, we investigate the main disadvantage of OFDM which is the high Peak to Average Power Ratio (PAPR) for both schemes, and compare between them. Photonic switching of a 4 Gbps 16-QAM UFMC and FBMC-OQAM signal centered at 50 GHz is performed. The optical single-sideband (OSSB) signal is generated with 18.85 dB of sideband suppression ratio (SSR). The results show that the best values of BER and

* Corresponding author at: Universiti Teknologi Malaysia, Malaysia, 81310, Johor Bahru, Johor, Malaysia.
E-mail addresses: amyazan1988@graduate.utm.my (Y. Alkhlefat), sevia@utm.my (S.M. Idrus), alfarabi@utm.my (F.M. Iqbal).

[1] The author Professor Ir Dr Sevia Mahdaliza Idrus is the Deputy Dean (Development & Alumni), Faculty of Engineering, UTM. She received her Bachelor in Electrical Engineering in 1998 and Master in Engineering Management in 1999, both from UTM. She obtained her Ph.D in 2004 from the University of Warwick, United Kingdom in optical communication engineering. She has served UTM since 1998 as an academic and administrative staff. Her main research interests are optical communication system and network, optoelectronic design, and engineering management. Her research output have been translated into a number of publications (H-indexed-11) and IPR including a high-end reference books, 'Optical Wireless Communication: IR Connectivity' published by Taylor and Francis, 49 book chapters and monographs, over 200 refereed research papers, 5 patents granted, 36 patent filings and holds 36 UTM copyrights. To date, she has secured and been involved in 38 research and consultation projects with a total value of RM114.2M. She is the founder and Director of a UTM spin-off company, iSmartUrus Sdn Bhd (1057063A) successfully commercialized her invention, a novel airtime based mobile micropayment solution and application-centric IoT based mobile enforcement device. She is Senior Member of IEEE and member of Editorial Board of few refereed international journals. She has been appointed as Guest Professor at Osaka Prefecture University and Tokai University, Japan in 2011 and 2014, respectively.

Peer review under responsibility of Faculty of Engineering, Alexandria University.

https://doi.org/10.1016/j.aej.2021.10.059

EVM can be obtained when the injection current (IC) is 0.7–0.9A. For converted signal using FBMC-OQAM, it has power penalty ~ 2.5 dB at BER threshold $1 \times 10^{-3}$and has also ~ 2 dB power penalty compared to the UFMC scheme at EVM threshold 5.6%. In addition, the wavelength switching system with FBMC and UFMC modulation schemes achieves the same PAPR.

1. Introduction

IN recent years we have witnessed an increase in the number of users of wireless communication systems, and in order to meet the user's requirements such as high data rate, high speed, and video streaming. These requirements it was necessary to find a solution that is manifested in the fifth generation (5G). In 5G, the expected number of connected devices and users will reach billion and it will provide different technologies such as the internet of things (IoT) and multiple-input multiple-output (MIMO) system [1]. In 4G, the modulation format was used is Orthogonal Frequency-Division Multiplexing (OFDM) and it has some drawbacks which make it difficult to be used in 5G and meet new requirements of users. The most apparent disadvantages of using OFDM in 5G are high Out of Band (OOB) power and high peak-to-average power ratio (PAPR) [2,3]. In 5G mobile systems, MMW signals and the doable modulation schemes such as universal filtered multicarrier (UFMC), filter-bank multicarrier (FBMC), filtered-OFDM (F-OFDM), and generalized frequency division multiplexing (GFDM), have been studied and investigated by many researcher in order to meet new user's requirements and avoid the aforementioned disadvantages of OFDM. These schemes have more powerful than cyclic prefix-OFDM (CP-OFDM) because of their low level of spectral side-lobe [4]. In this paper we are using two main modulation schemes which are UFMC and FBMC-OQAM.

1.1. Related works

Many researchers concentrate on wavelength conversion using SOA in the radio over fiber (RoF) systems. In [5], the authors experimentally demonstrated the MMW switching system using SOA for a 30 GHz MMW carrier signal to carry 3 Gbaud data rate using quadrature phase-shift keying (QPSK) signal and investigated the effects of main SOA's parameters. In [6], two cascaded SOAs have been used to switch 5G signal (25 GHz) and a 0.5 dB power penalty was achieved. In [7], a photonics-based microwave switching using SOA is proposed and experimentally demonstrated, where the 16-quadrature amplitude modulation (QAM) signal has a frequency of 20 GHz to carry 200 Mbps. To evaluate the conversion performance, the sideband suppression ratio (SSR) which is mean - the difference between the lower and upper sidebands - has been used. The SSR of the switched signal was 17.85 dB for switching based on up-conversion while it was 22.65 dB for down-conversion. In [8], the authors used VPI software to implement a wavelength conversion system for MMW FBMC signal using SOA to transmit 3Gbps over a carrier frequency of 30 GHz. This is done for two scenarios, the first one single FBMC signal and the second scenario with six aggregated signals in order to investigate such of this aggregation techniques with single and cascaded wavelength converters. In [9], the authors demonstrated experimentally the system of RoF downlink, using a cross polarization modulation (XPolM)-based all OSSB frequency up-conversion method in an SOA, with a 10-Gb/s 16QAM-OFDM signal at a carrier frequency of 60 GHz. In [10], an SOA has been used to convert the wavelength of MMW signal (30 GHz) which carrying 10 Gbps data rate of 16-QAM orthogonal frequency division multiplexing (OFDM) signal by using VPI software.

On the other side, the UFMC and FBMC have been investigated by many researchers and show their importance to be considered as the main modulation scheme for 5G. In [11], new reconfigurable architecture for UFMC transmitter has been proposed, which has features of low-complexity, flexibility to check the available filters and select one of them, and also can select a number of sub-carriers inside the subband without changes of resources of hardware. In [12], the authors designed a method of channel estimation and joint timing offset for multi-users UFMC uplink, the results show that this method can get more performance than existing approaches. In [13], the paper concentrates on designing and analyzing UFMC transceivers with a multi-antenna system that operating at MMW carrier frequencies, and it is providing a mathematical model for MIMO UFMC transceivers. The results show that these proposed algorithms are efficient and the data detector of the linear minimum mean-square error (MMSE) is able to reduce interference by removing guard times between consecutive packets which give 10%-13% of throughput gain. The authors in [14] proposed a precoding scheme and dynamic spectrum allocation scheme on the UFMC small cell system in order to reduce interference, the results show that the proposed schemes can mitigate the interference and reduce frequency offset's effect.

As in the UFMC, the FBMC has also received great attention from researchers. In [15], the schemes of adaptive modulation FBMC in RoF systems have been investigated, using experiments of scheduling techniques and bit loading, and then evaluated and compared the system performance with OFDM in both domains time and frequency. The experimental results show that FBMC has efficient performance which makes it suitable to be used in 5G. In [16], the authors studied FBMC in full-duplex carrier aggregation (CA) for MMWoF in heterogeneous mobile networks. The performance of the FBMC scheme surpasses OFDM in terms of EVM at the same value of received optical power, and single guard band spacing is needed while OFDM requires spacing of 26 sub-carriers to have free error transmission. Moreover, the results displayed that the seamless asynchronous aggregation of 12 FBMC and long-term evolution (LTE) signals. Besides, in [17], the authors experimentally demonstrated the MMWoF system of 5 CA FBMC sub-bands, and the results show that the system

achieved a data rate of 12 Gbps with 64-QAM signals by using offline digital signal processing.

1.2. Contribution

Most of the researchers concentrate on their research to compare UFMC and FBMC over the electrical link, not the optical link. On the other hand, many proposed literatures focused on wavelength conversion using standard modulation formats such as QPSK M−ary QAM and OFDM. So, there is a need to take into consideration that wavelength conversion using modulation formats that meeting the requirements of 5G networks. Our contribution is that we are proposing, analyzing, and comparing between two most common 5G modulation formats in the wavelength conversion systems using SOA.

1.3. Paper organization

The remainder of this paper is organized as follows:

Section II presents the basic model of UFMC and FBMC systems. In section III, a brief description of SOA and its nonlinear effects is provided. The system model and main parameters are explained in Section IV. The simulation comparison, analysis, and results are provided in Section V, and Section VI concludes the paper.

2. UFMC and FBMC SYSTEM model

2.1. UFMC

The UFMC system can be considered as a general form of OFDM but does not use a cyclic prefix (CP) [18], where the assigned bandwidth is divided into different sub-bands including a set of sub-carriers, then filter each sub-band using the finite impulse response (FIR) before transmitting [19,20]. This filtering process reduces and suppresses the levels of spectral side-lobe and then leading to gain higher robustness. As a result, the suppressed side-lobes minimize the inter-block interference (IBI) resulted from synchronization errors with no CP, which makes UFMC free from synchronization requirements and then offers it properly for higher spectral efficiency and more flexible resource allocation [21]. Moreover, when we compare UFMC with OFDM in terms of timing offsets (TO), UFMC is more robust in TO than OFDM. Also, UFMC has better performance of rejection OOB than OFDM, so that is why UFMC is a good proposed modulation scheme in 5G systems [22]. Fig. 1 shows the block diagram for the transmitter and receiver of the UFMC system.

The whole bandwidth of subcarriers (N) is divided into different sub-bands (B). Each sub-band includes a number of subcarriers (K) and not necessary all sub-bands need to be assigned for transmission. Then an N-pt IFFT is calculated for each sub-band and zeros inserted for each unallocated carrier. After that, the filter of each sub-band will be applied with a length of L and then sum all responses from all different sub-bands. The purpose of this filtering process is to reduce the OOB spectral emissions [23].

Fig. 1 illustrates the block diagram of the UFMC transceiver. At the transmitter side, each sub-band consists of subcarriers $K = N/B$. There are several methods to divide subcarriers such as random distribution or average. Theoretically, the carrier's number in the i-th sub-band is denoted by K_i , for i = 1, 2, . . . , B. for simplicity we considered that each sub-band contains the same number of subcarrier, so $K_i = K$, otherwise, $K_i \neq K$ but $\sum K_i = N$, for $i = 1, 2, \ldots, B$.

The analysis of UFMC is mentioned in [24]. Firstly, a generated information bits are mapped to different symbols using M−ary quadrature amplitude modulation (M−QAM) and these generated symbols are assigned to each sub-band by using the carrier average allocation method. In the frequency domain, the assigned symbols of the i-th sub-band are denoted by $\boldsymbol{S}_i$, with length $\boldsymbol{K}_i$. After that, these symbols are transformed into time domain signal s_i using N-point fast inverse Fourier transform (IFFT), but here there is a slight difference of IFFT from the conventional transformation. After that, the filtering process is applied to every single sub-band. It is worthy to note that, because of filter edge protection, UFMC relaxes the time synchronization requirements and improves the robustness of time and frequency misalignment.

After the filtering process of each sub-band, their responses will be summed together which will lead to generating discrete-time signals, so the superposition for symbols of all sub-bands in the time domain.

Assuming that all required channel's information can be obtained at the receiver. For received signals, RF operation and up-conversion are adopted. And because of noise interference, these band-pass signals are required to be converted into baseband signals. To demodulate these signals, the zero-padding process will be performed for received signals which can be done by filling a defined number of zeros beyond received signals, therefore, the length of received signals will be doubled of the transmitted signals, i.e. 2 N. then the 2 N-point FFT operation is performed.

On the receiver side, in order to eliminate the harmful effects of the channel, both equalization techniques can be used either time-domain equalization such as zero-forcing (ZF) equalization and minimum mean squared error (MMSE) equalization or frequency domain equalization, for instance, linear and nonlinear equalization. Generally, there is not too much difference in performance between time-domain equalization and frequency domain equalization.

2.2. FBMC/OQAM

The FBMC system is a multicarrier preferred scheme for 5G which reduces the OOB emissions and minimizes the requirements of synchronization [25]. In FBMC the filtering technique is applied for each sub-carrier in order to eliminate the signal's sidelobes [26]. FBMC has often used the offset quadrature amplitude modulation (OQAM) modulation format and the orthogonality must be applied only for neighboring subchannels in FBMC, not as OFDM which is applied for all carriers [27]. Fig. 2 illustrated the process of the FBMC transmitter and receiver. FBMC analysis is mentioned in [28].

Initially, the data bits are created and then symbol mapping is done with QAM format. In order to ensure the orthogonality and which leads to high spectral efficiency, the OQAM and Nyquist condition is used on the prototype filter. In OQAM precoding the complex data symbols (real and imaginary) are not transmitted at the same time where the imaginary part has a delay of half symbol duration [29,30]. Then a prototype filter was designed with overlapping factor $K = 4$. Assume that

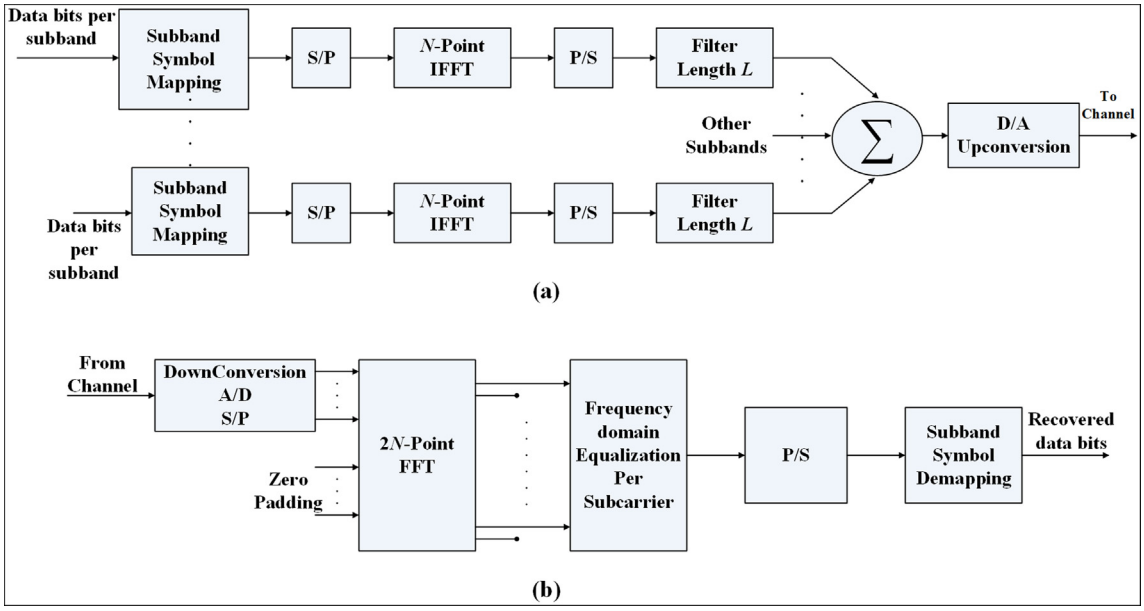

Fig. 1 UFMC block diagram (a) Transmitter. (b) Receiver.

the prototype filter's duration is $L = M \times K$ where M is the size of FFT, and K is an overlapping factor that describes a multiple of FFT size [31].

3. Semiconductor optical amplifier (SOA)

In recent years, optical amplifiers have attracted the attention of researchers because of their importance in various telecommunication systems such as wavelength division multiplexing (WDM) and radio over fiber (RoF) networks. There are many different types of optical amplifiers that are used frequently such as semiconductor optical amplifiers, Raman, and Erbium-doped fiber amplifiers (EDFA). SOA Attained importance from different advantages such as low cost, small size, and can be integrated with other modulators and semiconductors [32]. In addition, SOA has high gain and requires low input power and short time response [33]. The optical devices and optical networks have been seriously considered in 5G systems because of SOA's development which has displayed great success in various applications such as wavelength conversion [34], switching [35], power equalization [36], and logic operations [37]. SOA has nonlinear effects such as four-wave mixing (FWM), cross gain modulation (XGM), and self-phase modulation (SPM). These features are really very important and useful for the transparency of optical networks because no need to convert optical signals from optical to electrical domain and vice versa. In this paper, we utilize SOA in order to generate OSSB signal and convert 5G signals (UFMC and FBMC) from one wavelength to another desired one.

Fig. 3 displays the principle of all-optical wavelength conversion (AOWC) using SOA. Assume that we have two optical signals; one is that carrying a 5G signal which is called a Probe signal and the second is a pure laser which is called a Pump signal. The optical field of both signals can be described as following:

$$E_1(t) = A_1 exp(j\omega_1 t) \tag{1}$$

$$E_2(t) = A_2 exp(j\omega_2 t) \tag{2}$$

Where A_1 and A_2 represent the amplitude of probe and pump signals respectively, and ω_1 , ω_2 are the angular frequency for both signals respectively.

The optical field of the 5G continuous wave can be expressed by $E_0(t) = A_0 exp(j\omega_0 t)$ Where A_0 is the amplitude and ω_0 is the angular frequency. Then $E_0(t)$ is modulated by $V_{s1}(t)$ and $V_{s2}(t)$ through Mach-Zehnder Modulator (MZM). The mathematical model of MZM's output can be expressed as:

$$E_{out}(t) = \frac{E_{in}(t)}{10^{(IL/20)}} \left\{ (1-\gamma).exp\left[\frac{j\pi V_1(t)}{V_{\pi RF}} + \frac{j\pi V_{bias1}}{V_{\pi DC}}\right] + \gamma.exp\left[\frac{j\pi V_2(t)}{V_{\pi RF}} + \frac{j\pi V_{bias2}}{V_{\pi DC}}\right] \right\} \tag{3}$$

Where $E_{in}(t)$ represents the modulated light wave of laser which is the input of MZM; IL is the insertion loss; γ is the power ratio of both Y-branch waveguides, that is related to the modulator's extinction ratio; $V_1(t)$ and $V_2(t)$ are electronic modulation input signals of MZM with two channels; V_{bias1} and V_{bias2} are corresponding bias voltages of two channels; $V_{\pi RF}$ denotes switching modulation voltage; and $V_{\pi DC}$ denotes switching bias voltage.

Furthermore, we can deduce and find the mathematical model for modulated optical signals as the following:

$$E_{out}(t) = \frac{E_0(t)}{10^{(IL/20)}} \left\{ (1-\gamma).exp\left[\frac{j\pi V_{s1}(t)}{V_{\pi RF}} + \frac{j\pi V_{bias1}}{V_{\pi DC}}\right] + \gamma.exp\left[\frac{j\pi V_{s2}(t)}{V_{\pi RF}} + \frac{j\pi V_{bias2}}{V_{\pi DC}}\right] \right\} \tag{4}$$

Based on [38,39], the SOA's mathematical model can be written as:

$$E_{out\_SOA}(t) = E_{in\_SOA}(t).exp\left[\frac{|(1+j\delta).g(t).L|}{2}\right] \tag{5}$$

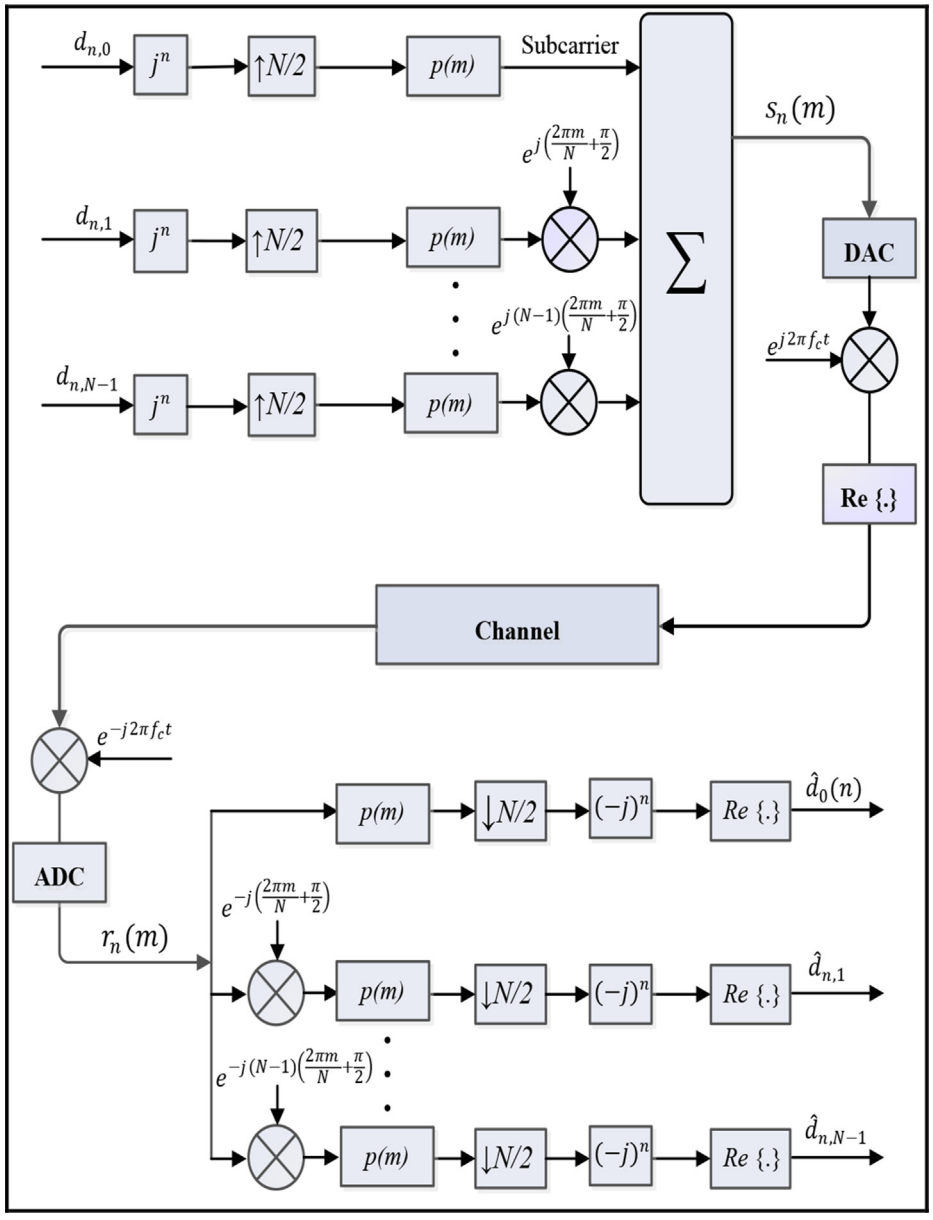

Fig. 2 OQAM/FBMC Communication System Model [29].

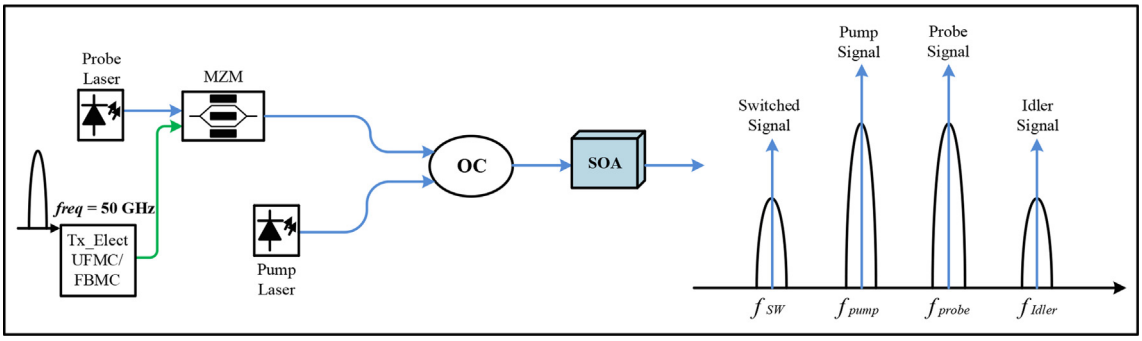

Fig. 3 Principle of the AOWC using SOA.

Where δ denotes line-width enhancement factor, $g(t)$ represents the net gain coefficient, and L is the SAO's length.

According to Fig. 3 and five equations 1–5, we can deduce and calculate SOA's output as following:

$$E_{out\_SOA}(t) = E_{1out\_coupler}.exp\left[\frac{|(1+j\delta).g(t).L|}{2}\right]$$

$$= \alpha^2\left[-jE_1(t).\sqrt{c(1-c)}+E_{out}(t).(1-c) - j\sqrt{c}E_2(t)\right]$$
$$exp\left[\frac{|(1+j\delta).g(t).L|}{2}\right]$$

$$= \alpha^2\left[-jA_1 exp(j\omega_1 t).\sqrt{c(1-c)} + \frac{exp(j\omega_0 t)}{10^{(IL/20)}}\right.$$
$$\left\{(1-\gamma).exp\left[\frac{j\pi V_1(t)}{V_{\pi RF}} + \frac{j\pi V_{bias1}}{V_{\pi DC}}\right] + \gamma.exp\left[\frac{j\pi V_2(t)}{V_{\pi RF}} + \frac{j\pi V_{bias2}}{V_{\pi DC}}\right]\right\}$$
$$\left.\times(1-c) - j\sqrt{c}A_2 exp(j\omega_2 t)\right] exp\left[\frac{|(1+j\delta).g(t).L|}{2}\right] \quad (6)$$

Where is the extra loss of the optical coupler and c is the coupling coefficient of the optical coupler.

As we can see from (6), the SOA's output optical field is related directly to ω_0, ω_1 and ω_2, where there are different nonlinear relations between themselves. So, the frequencies of new two generated signals (let's call them switched and idler) due to the FWM effect can be written as $f_{sw} = 2f_{Pump} - f_{Probe}$

And $f_{idler} = 2f_{Probe} - f_{Pump}$ respectively. As stated in [7], the

optical field of the switched signal at ω_{SW} can be written as:

$$E_{sw} = -\frac{1}{2}\left[\frac{1-i\delta}{1-i\omega_d\tau_c}\cdot\frac{1}{I_s} + \frac{1-i\beta}{1-i\omega_d\tau_n}\cdot\frac{1}{I_n}\right] \times \left|E_{Pump}\right|^2 E^*_{Probe} \quad (7)$$

where $\omega_d = \omega_{Pump} - \omega_{Probe}$ is the frequency detuning, τ_c and τ_n are the relaxation time constants for carrier density modulation and nonlinear gain, I_s and I_n are the saturation powers for carrier density modulation and nonlinear gain and β represents the ratio of imaginary and real parts of the nonlinearity gain induced change of refractive index. It is noted that the FWM's generation comes from the carrier density modulation and nonlinear gain and the switched signal is the replica of the probe signal with conjugated phase. At the same time, the probe signal experiences the nonlinear effect of SOA

which is SPM presenting a phase difference (ϕ) between the components of frequency in the phase ($\sim\sin(\Omega_m t + \phi)$) and that in the amplitude ($\sim\sin(\Omega_m t)$). [40,41]. Considering SPM effect in SOA, (7) can be expressed as :

$$E_{sw} = -\frac{1}{2}\left[\frac{1-i\delta}{1-i\omega_d\tau_c}\cdot\frac{1}{I_s} + \frac{1-i\beta}{1-i\omega_d\tau_n}\cdot\frac{1}{I_n}\right]$$
$$\times \left|E_{Pump}\right|^2.E_0\left[1+\frac{m}{2}sin(\Omega_m t)\right]$$

$$\times exp\left\{-i[\omega_{sw}t + \frac{m}{2}sin(\Omega_m t + \phi)]\right\} \quad (8)$$

where $E0$ is the carrier's amplitude, ε is the chirp parameter of the SPM and m is the RF modulation index. Based on [40], at high frequencies, the value of ϕ is close to $\pi/2$, so the modulation of OSSB the switched carrier ω_{sw} is performed. Accordingly, the RF signal is converted from the optical carrier of probe signal into optical carrier od switched signal ω_{sw} by using the nonlinear effects of SOA FWM and SPM.

From (8), we can see that ϕ is determining the SSR of the OSSB switched signal. When ϕ equals to $\pi/2$, OSSB can be achieved (one sideband is totally suppressed), and when ϕ is not close to $\pi/2$, the SSR is decreasing. According to [41], ϕ can be written as:

$$\phi = \pi - arctan(\Omega_m.\tau_{eff}) \quad (9)$$

where τ_{eff} is the effective recovery time of SOA. For a specific value of τ_{eff} and large value of Ω_m , the value of ϕ will be close enough to $\pi/2$, then the larger value of SSR will be achieved.

4. Simulation model

Fig. 4 displays the proposed system model for wavelength conversion of 5G signal UFMC/FBMC using SOA. This model consists of three sections: the transmitter (Central Office), wavelength converter, and finally the receiver. The CO includes the electrical 5G signal (UFMC/FBMC) with 4 Gbps data rate and laser diode (LD) which is considered as the main carrier and operating at a specified wavelength (1549.32 nm). The RF frequency is set for 50 GHz MMW carrier. The MZM is used to combine the RF signal (UFMC/FBMC) with the optical carrier and produce the optical double-sideband signal (ODBS) which is called a probe signal. After amplification of probe signal, it is entering to the WC stage with pump laser optical signal which is operating at a specified wavelength (1547.72 nm) and then launched with probe signal to the optical coupler (OC) with 50:50 percent. The resulted signal is launched to SOA. Then we exploited the nonlinear effects of SAO in order to generate an OSSB signal and convert the 5G signal into a new wavelength which is named a switched signal. For analysis, a bandpass filter is used to select the desired signal from SOA's output.

The switched signal can be detected using the photodetector (PD) which generates back the UFMC/FBMC signals over the original transmitted RF carrier frequency (50 GHz). On the receiver side, we implemented a UFMC/FBMC demodulator to compare the wavelength conversion performance for both 5G signals. Table 1 summarizes the main simulation parameters.

5. Simulation results and analysis

The OSSB wavelength conversion process based-MMW switching is achieved. The probe's wavelength is fixed at 1549.32 nm and power 2.38 dBm while the pump's wavelength is fixed at 1547.72 nm and power 2.04 dBm, so the wavelength spacing ($\Delta\lambda$) between probe and pump is 1.6 nm. If the wavelength of switched signal (λ_{sw}) after conversion is shorter than the wavelength of probe signal (λ_{Probe}) then the wavelength down-conversion is performed. A 4-Gbps 16-QAM UFMC signal is modulated on probe laser. The injection current of SOA is set at 0.9 A.

After that, both optical signals (probe and pump) being launched into SOA, the nonlinear effects (FWM, SPM) of SOA will result in OSSB generation and wavelength conversion. Indeed, we had the plan to compare between UFMC and FBMC under the same conditions, but the simulation results show that both outputs are the same in terms of SSR and SOA's behavior,

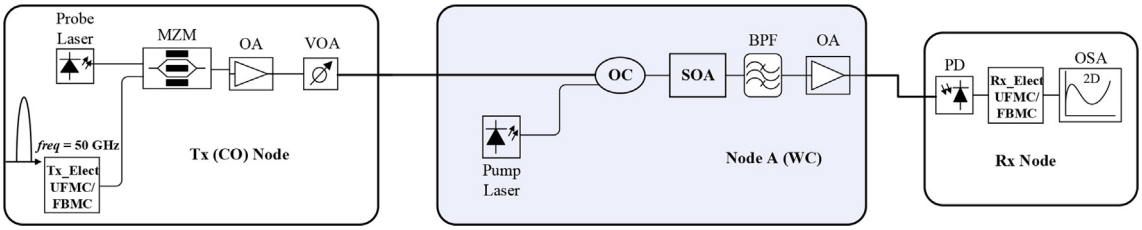

Fig. 4 Simulation Setup for wavelength conversion of UFMC/FBMC signals using SOA. MZM: Mach-Zehnder modulator, OA: optical amplifier, VOA: variable optical attenuator. OC: optical coupler, SOA: semiconductor optical amplifier, BPF: band pass filter, PD: photodetector, and OSA: optical spectrum analyzer.

Table 1 Main System Parameters.

Parameter	Value	Unit
Signal Type	UFMC/FBMC-OQAM	–
Order	16-QAM	–
Number of Carriers	256	–
SRRC Roll-off factor	0.18	–
Signal Data Rate	4	Gbps
Probe Signal Wavelength	1549.32	Nm
Probe Signal Power	2.38	dBm
Pump Signal Wavelength	1547.72	Nm
Pump Signal Power	2.04	dBm
RF Carrier Frequency	50	GHz
RF Power	0	dBm
SOA Parameters		
Injection Current	0.9	A
Length	5.00E-04	M
Width	3.00E-06	M
Height	8.00E-08	M
Optical confinement factor	0.15	–
Waveguide loss coefficient	4000	1/m

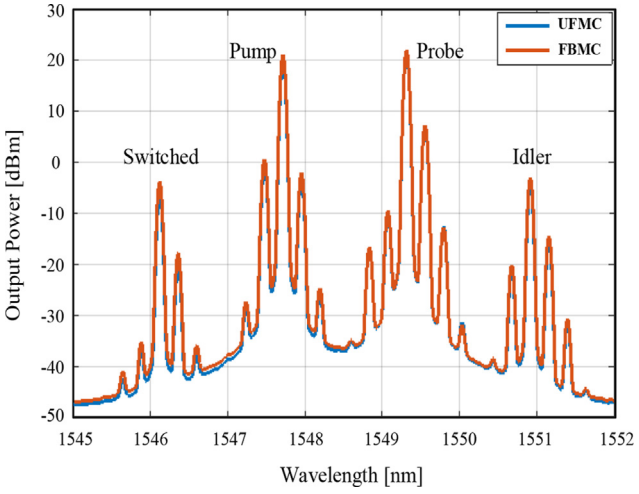

Fig. 5 Measured optical power spectrum at the output of SOA for UFMC and FBMC.

as shown in Fig. 5 which displays the optical spectrum of the output of SOA when 4-Gbps 16-QAM UFMC/FBMC-OQAM signal centered at 50 GHz. This is agreed with the fact saying that the SOA is transparent to the modulation format as mentioned in [5]. As we can see, the carried information by probe signal is copied successfully to new switched signal with wavelength 1546.12 nm which is also an OSSB signal. If we have a WDM system then the information will be converted to a new channel which covers wavelength 1546.12 nm, so by adjusting the wavelength of probe and pump signals, we can obtain different wavelengths which carrying RF signal and then it can be directed to new WDM channels. Accordingly, millimeter wave switching is implemented.

In the next step, we investigated the generation of OSSB signal based on nonlinear effect SPM in SOA. It is done by disconnecting the pump signal and injecting only the probe signal into SOA. In order to see the effect of modulating RF frequency on the SSR, we changed the RF frequency with three values 30, 40, and 50 GHz.

The measured optical spectrum with SSR values is shown in Fig. 6. As we can notice, the OSSB signals are generated, and the resulted SSR for three OSSB signals with frequencies 30, 40, and 50 GHz are 9.75, 12.78, and 19.95 dB respectively which is increases with the increment of RF frequency. These results agree with the relationship between Ω_m and ϕ in (9) proving that the amplitude and phase terms of the frequency component have a difference in phase with a value of $\pi/2$ which is resulted due to SPM effect in SOA [40,41].

Fig. 7 shows the measured optical spectrum of the switched signal at wavelength 1546.12 nm with SSR is equal to 18.85 dB. It is including also the constellation diagram with an EVM of 5.27%. If we compare the SSR (with same RF frequency) in Fig. 6 (c) (19.95 dB) and Fig. 7 (18.85 dB), it is smaller $\sim$ 1.1 dB in the case of both probe and pump injected to SOA due to existing of pump signal changes the SOA's carrier density which gives different ϕ in (8).

After that we compared two scenarios of the UFMC system in terms of EVM; one with switching (wavelength conversion) and the other without switching (back-to-back) as shown in Fig. 8. It shows the values of EVM versus received optical power. When we are applying the EVM threshold of 5.6% [42], the resulted power penalty that makes received optical power increased in order to have the same value of EVM is 2.25 dB. Therefore, if we have to obtain the same RF power with the same OSNR, more optical power is required for the OSSB system compared with the DSB system.

Fig. 9 displays the BER measurements without switching (B2B) and with switching for UFMC system, the results show 2.4 dB BER penalty at threshold BER 1×10^{-3} [43]. The low power penalty between B2B and switched signal can be attrib-

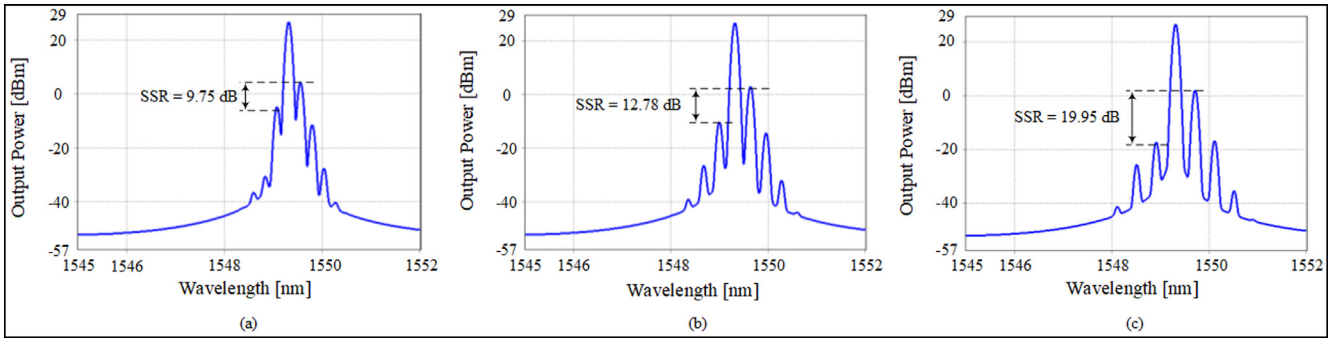

Fig. 6 Measured SSR for probe signal at 1549.32 nm carrying an RF signal with a frequency of (a) 30, (b) 40, and (c) 50 GHz after the SOA when the pump signal is disconnected.

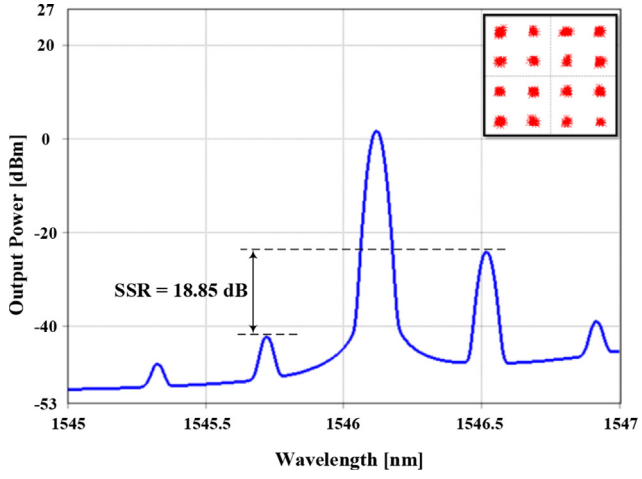

Fig. 7 Measured BER values versus received optical power without and with UFMC MMW switching based on wavelength down-conversion.

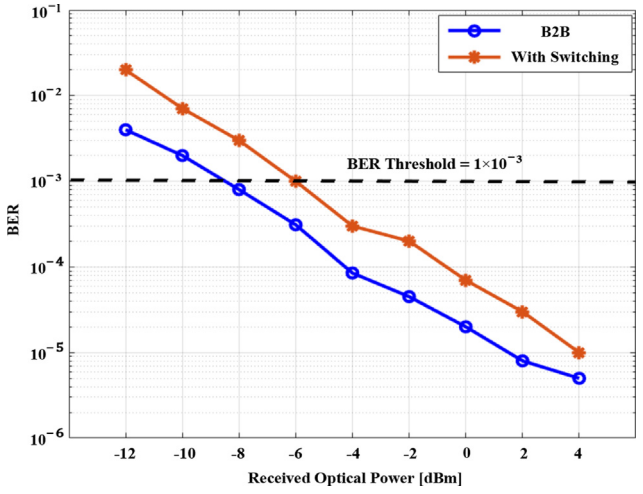

Fig. 9 Measured EVM values versus received optical power without and with UFMC MMW switching based on wavelength down-conversion.

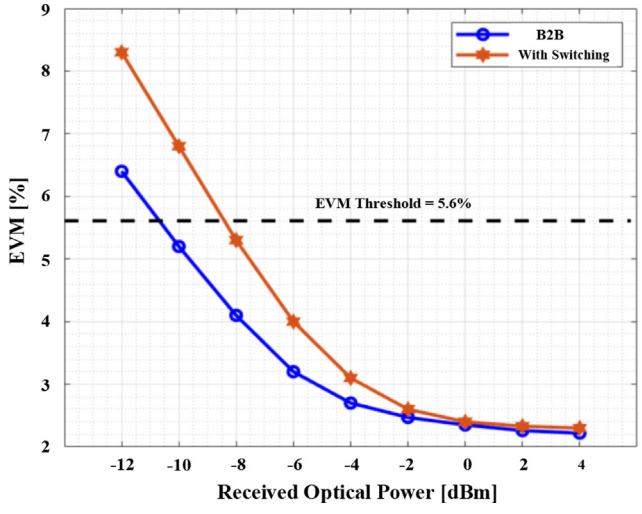

Fig. 8 The measured optical spectrum of the switched signal at a wavelength of 1546.12 nm for UFMC. Inset: measured constellation diagram.

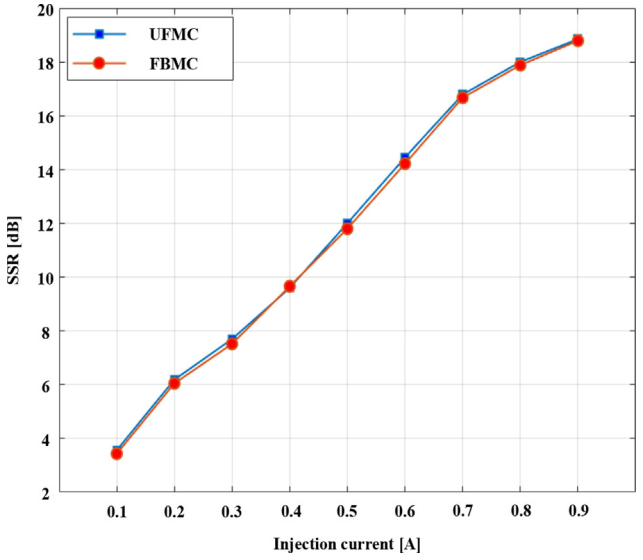

Fig. 10 Measured SSR versus Injection Current for UFMC and FBMC.

uted to the fact saying that the nonlinear effects of SOA are not dominant. So, the SOA can be considered to be a suitable solution for wavelength conversion.

Fig. 10 shows the effect of injection current on the SSR for both schemes UFMC and FBMC. It can be seen when the injection current increased, the SSR increased accordingly and the UFMC and FBMC give almost the same results. The maximum SSR can be obtained at 0.9 A.

In the next step, the relationship between EVM and the injection current of SOA for UFMC and FBMC is investigated as shown in Fig. 11. From this figure, the EVM values for both schemes are greatly decreased with increasing the SOA's injection current.

Furthermore, we can notice that the UFMC scheme is giving better performance than the FBMC scheme in terms of injection current. From both Figs. 10 and 11, we can notice that the optimum values of EVM can be obtained when the Injection current is within the range of 0.7 to 0.9 A.

In Fig. 12 (a) and (b) we show the switching performance in terms of BER and EVM respectively versus OSNR for UFMC and FBMC. It can be seen from Fig. 12 (a) that UFMC has better BER than FBMC with ~2.5 dB at BER threshold 1× while the FBMC scheme has a ~2 dB power penalty compared to the UFMC scheme at an EVM threshold of 5.6% as shown in Fig. 12 (b). In addition, we notice that both schemes have better performance when OSNR value increased and the recommended values of OSNR are above 30 dB.

The main disadvantage of multicarrier modulation formats is the high peak to average power ratio (PAPR). Where the input data is divided into many subcarriers and these subcarriers are independently modulated at different carrier frequencies then added up at the same time for transmission aim which produces high PAPR.

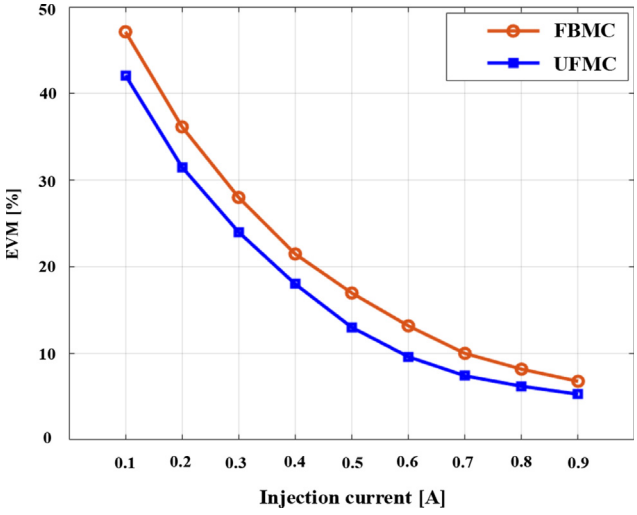

Fig. 11 Measured EVM versus Injection Current for UFMC and FBMC.

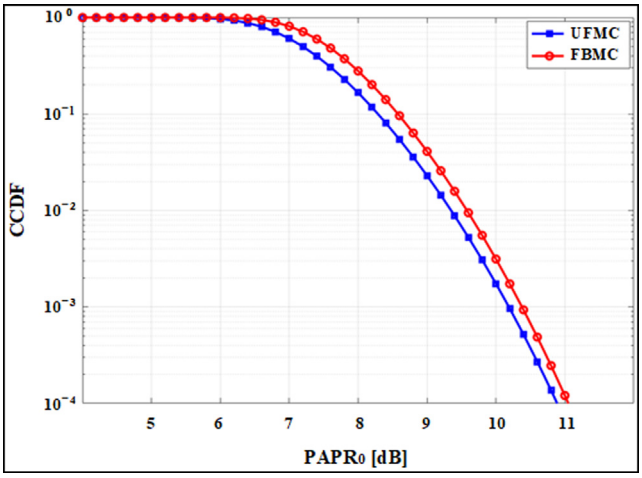

Fig. 13 The measure of complementary cumulative distribution function (CCDF) of PAPR for UFMC and FBMC.

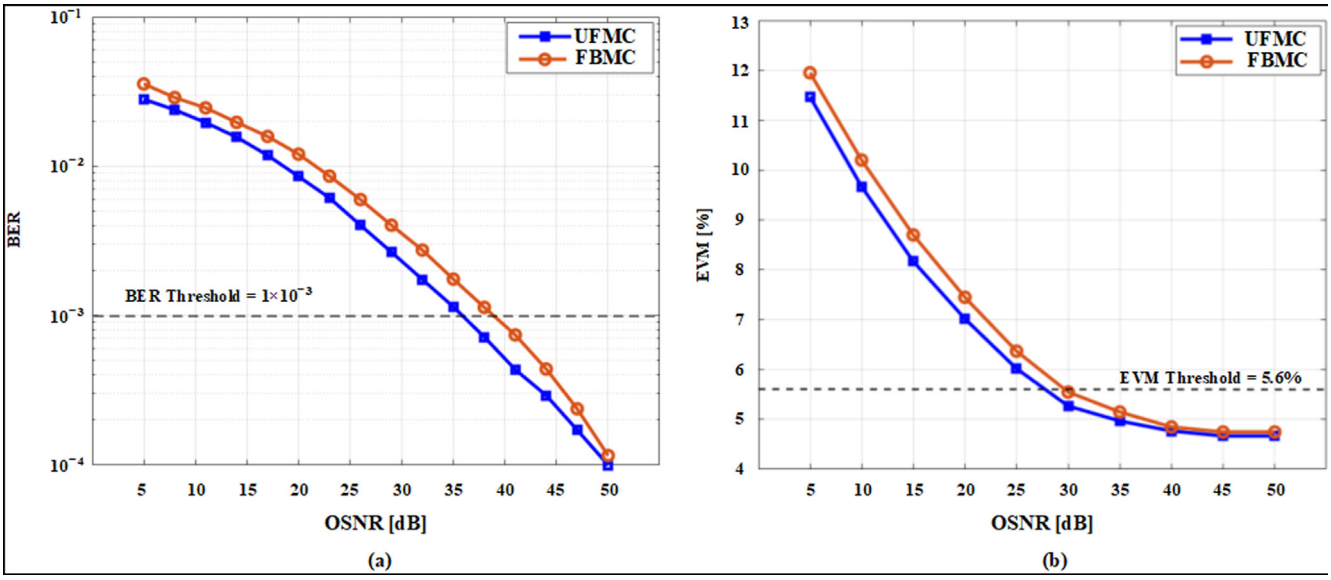

Fig. 12 Measured (a) BER and (b) EVM versus OSNR for UFMC and FBMC.

The peak power has resulted when many signals are added to each other in the same phase, and also when many signals are equal times of the signal's average power. Therefore, the PAPR is high in the multicarrier system [44].

Fig. 13 displays the complementary cumulative distribution function (CCDF) versus $PAPR_0$ for UFMC and FBMC. CCDF can be defined as the probability that exceeds a specific value of $PAPR_0$. From Fig. 13, the PAPR at CCDF = $1 \times 10^{-3}$for UFMC and FBMC is almost the same [45].

6. Conclusions

This paper implements a photonic Millimeter-wave switching and OSSB wavelength conversion using SOA for 5G modulation formats UFMC and FBMC-OQAM. This is done using MATLAB and virtual photonic integrated (VPI) software. The fast response of the nonlinear effect of SOA (i.e. FWM and SPM) provides a fast switching speed. A 4-Gbps 16-QAM UFMC/FBMC-OQAM signal centered at carrier frequency 50 GHz is switched to new desired wavelength using simulation of VPI and we investigated the performance of it by the resulted SSR which is 18.85 dB. We investigated the system with and without switching for both UFMC/FBMC-OQAM signal in terms of BER and EVM and the simulation results show that power penalty is $\sim$ 2.4 dB when we use wavelength conversion system compared with the B2B system. Also, we studied the effect of SOA's injection current (IC) on SSR, BER, and EVM for both schemes, the results give almost the same SSR for UFMC and FBMC-OQAM while giving better BER and EVM for UFMC compared to FBMC-OQAM. In addition, the best values of BER and EVM can be obtained when IC is 0.7–0.9A. For the converted signal using FBMC-OQAM, It has a power penalty of $\sim$ 2.5 dB at BER threshold $1 \times 10^{-3}$and has also $\sim$ 2 dB power penalty compared to the UFMC scheme at EVM threshold 5.6%. Finally, we investigated PAPR for both modulation formats, the results show that the wavelength switching system with UFMC and FBMC modulation scheme achieves the same PAPR value.

Declaration of Competing Interest

The authors declare that they have no known competing financial interests or personal relationships that could have appeared to influence the work reported in this paper.

Acknowledgements

This work is supported by Universiti Teknologi Malaysia institutional grant 08G49 and is part of a collaborative project with a photonic Laboratory (KACST-TIG-RFTONIC-KSU). The authors would like to thank Universiti Teknologi Malaysia and King Saud University for their cooperation.

References

[1] L. Chettri, R. Bera, A comprehensive survey on Internet of Things (IoT) toward 5G wireless systems, IEEE Internet Things J. 7 (1) (2020) 16–32.
[2] V. Sudha, D. Sriram Kumar, Low complexity PAPR reduction in SLM-OFDM system using time domain sequence separation, Alexandria Eng. J. 57 (4) (2018) 3111–3115.
[3] A. Kumar, M. Gupta, A review on activities of fifth generation mobile communication system, Alexandria Eng. J. 57 (2) (2018) 1125–1135.
[4] A.F. Almutairi, M. Al-Gharabally, A. Krishna, Performance analysis of hybrid peak to average power ratio reduction techniques in 5G UFMC systems, IEEE Access 7 (2019) 80651–80660.
[5] Saadaoui, F., et al., Optimizing OSSB generation using semiconductor optical amplifier (SOA) for 5G millimeter wave switching. IEEE Access, 2017. **5**: p. 6715-6723.
[6] M.A. Esmail, A. Ragheb, H. Fathallah, S. Alshebeili, Demonstration of photonics-based switching of 5G signal over hybrid all-optical network, IEEE Photonics Technol. Lett. 30 (13) (2018) 1250–1253.
[7] D. Zhu, Z. Wei, H. Wu, S. Pan, Photonics-based microwave switching using optical single sideband wavelength conversion in a semiconductor optical amplifier, IEEE Trans. Microw. Theory Tech. 65 (1) (2017) 245–252.
[8] Y. Alkhlefat et al, Millimeter wave switching for single carrier and aggregated filter bank multi-carrier signals in radio over fiber networks, Opt. Fiber Technol. 60 (2020) 102335.
[9] S.-H. Lee, J.-I. Song, An XPolM-based all-optical SSB frequency up-conversion technique in an SOA, IEEE Photonics Technol. Lett. 29 (7) (2017) 627–630.
[10] Alkhlefat, Y.A., et al. Millimeter Wave Switching in Radio over Fiber Networks using Semiconductor Optical Amplifier (SOA). in 2018 21st Saudi Computer Society National Computer Conference (NCC). 2018. IEEE.
[11] V. Kumar, M. Mukherjee, J. Lloret, Reconfigurable architecture of UFMC transmitter for 5G and its FPGA prototype, IEEE Syst. J. 14 (1) (2020) 28–38.
[12] Y. Xu, H. Chu, X. Wang, Joint timing offset and channel estimation for multi-user UFMC uplink, IEEE Wireless Commun. Lett. 9 (2) (2020) 236–239.
[13] S. Buzzi, C. D'Andrea, D. Li, S. Feng, MIMO-UFMC transceiver schemes for millimeter-wave wireless communications, IEEE Trans. Commun. 67 (5) (2019) 3323–3336.
[14] L. Wu, Z. Zhang, J. Dang, B. Zhu, H. Jiang, H. Liu, UFMC-based interference management for heterogeneous small-cell networks, IEEE Access 7 (2019) 136559–136567.
[15] Xu, M., et al. Investigation of FBMC in mobile fronthaul networks for 5G wireless with time-frequency modulation adaptation. in 2016 Optical Fiber Communications Conference and Exhibition (OFC). 2016. IEEE.
[16] J. Zhang, M. Xu, J. Wang, F. Lu, L. Cheng, H. Cho, K. Ying, J. Yu, G.-K. Chang, Full-duplex quasi-gapless carrier aggregation using FBMC in centralized radio-over-fiber heterogeneous networks, J. Lightwave Technol. 35 (4) (2017) 989–996.
[17] H.N. Parajuli, H. Shams, L.G. Gonzalez, E. Udvary, C. Renaud, J. Mitchell, Experimental demonstration of multi-Gbps multi sub-bands FBMC transmission in mm-wave radio over a fiber system, Opt. Express 26 (6) (2018) 7306, https://doi.org/10.1364/OE.26.007306.
[18] J. Wen, J. Hua, W. Lu, Y.u. Zhang, D. Wang, Design of waveform shaping filter in the UFMC system, IEEE Access 6 (2018) 32300–32309.
[19] Ahmed, S.R., A.S. Abdullah, and N.M. Hammash. *Universal Filtered Multicarrier (UFMC) vs. Orthogonal Frequency Division Multiplexing (OFDM)*. in *Journal of Physics: Conference Series*. 2020. IOP Publishing.
[20] M.I. Al-Rayif, H.E. Seleem, A.M. Ragheb, S.A. Alshebeili, PAPR Reduction in UFMC for 5G Cellular Systems, Electronics 9 (9) (2020) 1404, https://doi.org/10.3390/electronics9091404.
[21] H. Fourati, R. Maaloul, L. Chaari, A survey of 5G network systems: challenges and machine learning approaches, Int. J. Mach. Learn. Cybern. 12 (2) (2021) 385–431.

[22] A. Kumar, R. Dhanagopal, M.A. Albreem, D.-N. Le, A comprehensive study on the role of advanced technologies in 5G based smart hospital, Alexandria Engineering Journal 60 (6) (2021) 5527–5536.
[23] Schaich, F., T. Wild, and Y. Chen. Waveform contenders for 5G-suitability for short packet and low latency transmissions. in 2014 IEEE 79th Vehicular Technology Conference (VTC Spring). 2014. IEEE.
[24] S. Wei, H. Li, W. Zhang, W. Cheng, A comprehensive performance evaluation of universal filtered multi-carrier technique, IEEE Access 7 (2019) 81429–81440.
[25] S.O. Tiwari, R. Paulus, FBMC OQAM: novel variant of OFDM, J. Optical Communications (2021).
[26] Dalela, P.K., et al. Beam Division Multiple Access (BDMA) and modulation formats for 5G: Heir of OFDM? in 2018 International Conference on Information Networking (ICOIN). 2018. IEEE.
[27] G. Femenias, F. Riera-Palou, X. Mestre, J.J. Olmos, Downlink scheduling and resource allocation for 5G MIMO-multicarrier: OFDM vs FBMC/OQAM, IEEE Access 5 (2017) 13770–13786.
[28] Zakaria, R., *Transmitter and receiver design for inherent interference cancellation in MIMO filter-bank based multicarrier systems*. 2012, Conservatoire national des arts et metiers-CNAM.
[29] Jiang, T., et al., OQAM/FBMC for future wireless communications: Principles, technologies and applications. 2017: Academic Press.
[30] M. Bellanger et al, FBMC physical layer: a primer, PHYDYAS 25 (4) (2010) 7–10.
[31] Ravindran, R. and A. Viswakumar. Performance evaluation of 5G waveforms: UFMC and FBMC-OQAM with Cyclic Prefix-OFDM System. in 2019 9th International Conference on Advances in Computing and Communication (ICACC). 2019. IEEE.
[32] D. Huang, *Semiconductor optical amplifiers and related applications*. in *Applications of Photonic Technology 5*, International Society for Optics and Photonics, 2003.
[33] A. Bogoni, L. Poti, C. Porzi, M. Scaffardi, P. Ghelfi, F. Ponzini, Modeling and measurement of noisy SOA dynamics for ultrafast applications, IEEE J. Sel. Top. Quantum Electron. 10 (1) (2004) 197–205.
[34] Y. Liu, E. Tangdiongga, Z. Li, H. de Waardt, A.M.J. Koonen, G.D. Khoe, X. Shu, I. Bennion, H.J.S. Dorren, Error-free 320-Gb/s all-optical wavelength conversion using a single semiconductor optical amplifier, J. Lightwave Technol. 25 (1) (2007) 103–108.
[35] H. Kawaguchi, *All-Optical Switching of Picosecond Pulses by Four-Wave Mixing in a Semiconductor Optical Amplifier*. IPAP Books 2, Photonics Based on Wavelength Integration and Manipulation (2005) 271–282.
[36] B.S. Gopalakrishnapillai, M. Premaratne, A. Nirmalathas, C. Lim, Power equalization using polarization rotation in semiconductor optical amplifiers, IEEE Photonics Technol. Lett. 17 (8) (2005) 1695–1697.
[37] G. Berrettini, A. Simi, A. Malacarne, A. Bogoni, L. Poti, Ultrafast integrable and reconfigurable XNOR, AND, NOR, and NOT photonic logic gate, IEEE Photonics Technol. Lett. 18 (8) (2006) 917–919.
[38] Agrawal, G.P. and N.K. Dutta, *Rate equations and operating characteristics*, in *Semiconductor Lasers*. 1993, Springer. p. 231-318.
[39] Shimada, S. and H. Ishio, *Optical amplifiers and their applications*. 1994: John Wiley & Son Ltd.
[40] U.-S. Lee, H.-D. Jung, S.-K. Han, Optical single sideband signal generation using phase modulation of semiconductor optical amplifier, IEEE Photonics Technol. Lett. 16 (5) (2004) 1373–1375.
[41] H. Jiang, H. Wen, X. Zheng, Z. Liu, K. Wang, H. Zhang, Y. Guo, Improved optical single-sideband generation using the self-modulation birefringence difference in semiconductor optical amplifiers, Opt. Lett. 32 (17) (2007) 2580, https://doi.org/10.1364/OL.32.002580.
[42] D. Zhu, S. Liu, S. Pan, Multichannel up-conversion based on polarization-modulated optoelectronic oscillator, IEEE Photonics Technol. Lett. 26 (6) (2014) 544–547.
[43] A.A.E. Hajomer, M. Presi, N. Andriolli, C. Porzi, W. Hu, G. Contestabile, X. Yang, On-chip all-optical wavelength conversion of PAM-4 signals using an integrated SOA-based turbo-switch circuit, J. Lightwave Technol. 37 (16) (2019) 3956–3962.
[44] Thiyagarajan, S. and S. Veerappan, *Performance Analysis of UFMC and its Comparison with CP-OFDM*.
[45] Y. Medjahdi, S. Traverso, R. Gerzaguet, H. Shaiek, R. Zayani, D. Demmer, R. Zakaria, J.-B. Dore, M. Ben Mabrouk, D. Le Ruyet, Y. Louet, D. Roviras, On the road to 5G: Comparative study of physical layer in MTC context, IEEE Access 5 (2017) 26556–26581.